



GAIN-PHASE MARGINS BASED STABILITY ANALYSIS OF TIME DELAYED HYBRID LOAD FREQUENCY CONTROL SYSTEM

HALIL EROL¹, SAFFET AYASUN²

Key words: Hybrid power systems, Microgrids, Power system stability, Renewable energy sources, Smart grids.

The stability analysis of a hybrid load frequency control (LFC) system with communication delays is presented comprehensively in this paper. Stability analysis, which contains delays, is done by using an exact and a direct analytical method. In the computation of delay margins gain and phase margins are also taken into account. Hybrid LFC schemes installed with proportional-integral (PI) controllers is carried out in case studies. In this method stability and relative stability regions are obtained. Also, the stability boundary curves are obtained as a function of the PI controller parameters. Gain and phase margins can be selected by considering time delay margin suitable with the controller gains for robustness purposes.

The main purpose of this paper is to provide information for time delay of hybrid LFC system and determine the boundaries of constant phase margin and gain margin in a parameter space or a parameter plane. Then, the effects of adjustable parameters can be clearly defined. The time-domain simulation studies are carried out which indicate that results are convenient.

1. INTRODUCTION

The demand to renewable energy in micro grid systems is growing due to environmental warming, rising fuel prices and pollution. The global warming that is partially caused by thermal power generators is an international environmental concern, which has become a decisive factor in energy planning [1]. Moreover, as the power systems power capacity enlarges, controllability of system getting harder. For that reason, utilities tend to use hybrid micro grids in some countries. Taking this problem into account and as a remedial measure, strong support is expected from renewables due to competitive power prices of solar and wind farms [2]. Also, to supply electricity to the remotely located communities by extending the conventional utility grid is uneconomical [3]. The wind-PV hybrid energy system with the support of battery bank and a diesel generator as a back-up would be an economical choice to supply electricity to remotely located areas. To feed remote areas from central power grid would be uneconomical because of high installation costs. Moreover, due to high cost of fuel, the renewable energy in grid independent system is getting more popular. The smart local grids are optimum solution to the present-day power sector disadvantages [4]. These are grid losses, pollution of environment caused by typical thermal power generation. Also, in rural areas, accessibility and reliability of power is poor [5]. Most reliable renewable power generation technologies are solar and wind power generation. Because, solar and wind power technology has considerable share in power production era. Also, the production costs of these systems getting lower and lower day by day. Disadvantage of these power systems is that, output of these systems may change with climate, seasons, dirtiness etc. Since power output of these systems are not constant for all times, some form of energy storage or sometimes additional generation is needed. Because of weather condition variation, there has been power fluctuations at the output of solar and wind resources. To overcome this drawback, battery bank and FC systems are generally integrated to hybrid power systems to

stabilize the output of the hybrid power systems [6]. To obtain maximum efficiency from the hybrid power system, the design and operation part should be implemented appropriately [7]. Control setting, operating strategies and sizing are interdependent in these systems. In addition, some parts of the system components characteristic behavior is non-trivial. For that reason, planning a hybrid system for a specific location that meets different design possibilities becomes quite difficult. The schematic diagram of a typical PV–wind, diesel generator hybrid system is shown in Fig. 1. A cascade sliding mode controller without current control loop in a micro grid system is proposed in [8]. Time delay of two and three area decentralized power systems are analyzed in [9] with respect to robustness of PI controller. H_∞ stability analysis of Networked Control Systems with uncertain discrete-time is investigated in [10] and an iterative algorithm is developed to compute the controller's parameters by means of the Cone Complementarity Linearization Method. In islanded micro-grid, the stability analysis of load frequency control system with the presence of the time delay using linear matrix inequality method is presented in [11]. For computing the maximum value of the time-delays, in which the LFC system remains asymptotically stable by using Lyapunov–Krasovskii functional method, is proposed in [12]. In this study, linear matrix inequality formulation is used. Another load frequency control (LFC) scheme with dumped load (DL) approach is analyzed in [13].

In this paper, delay dependent micro grid power system is analyzed and it is shown in Fig. 1. It includes different types of power sources such as solar PV panel, wind turbine, ultra-capacitor, diesel generator and fuel cell. The ultra-capacitor (UC) is used for excess energy storage. Excessive energy generated by the generating subsystems is stored in UC and it is assumed that it has enough capacity. The load generally consists of residential or small-scale industrial loads [14].

Time delays have become a great concern in frequency control of power systems since they reduce the effectiveness of controllers and sometimes may cause instability [15]. The

¹ Electrical and Electronics Engineering Department, Osmaniye Korkut Ata University, Osmaniye, 80000, Turkey.
halilerol@osmaniye.edu.tr (Corresponding author)

² Electrical and Electronics Engineering Department, Gazi University, Ankara, 06240, Turkey

frequency variation in the system is sensed by sensors and this signal is sent to the controller. This process takes place in some time and causes some delay. Because of these delays between production unit and controller, influence system dynamics. In addition to this, it may derive the hybrid power system into unstable position [16–19]. The modeling of hybrid renewable energy system and frequency deviation control is investigated in a lot number of literatures. Some of them are the small signal stability analysis of a hybrid power generation/storage system connected to isolated load is reported by Dong Jing and Lee Wang [16,17]. Reduced dump load technique is used for analyzing the load frequency control of an isolated small-hydro power plant is investigated by S. Doolla and T.S. Bhatti, in [20]. Dynamic model of FCs is simulated as first order lead lag compensator in [21]. To the best of our knowledge, frequency deviation control with time delay in hybrid renewable energy systems has not been used in the context of phase and gain margin. Thus, to the best of our knowledge, this study is the first application of frequency deviation control with time delay in hybrid renewable energy systems to determine the range of phase and gain margin.

Generally, stability is considered as marginal stability in delay margin computations [22,23]. In power systems taking additional load or losing load may cause frequency deviation. Due to unacceptable oscillations in the frequency, a practical hybrid LFC system cannot operate near such points. Therefore, in hybrid LFC system, first of all, the stability condition must be met. In addition to this, dynamic performance (i.e., damping, steady-state error, settling time, etc.) of the system should be met. To achieve these design goals phase and gain margins must be taken into consideration in delay margins computation.

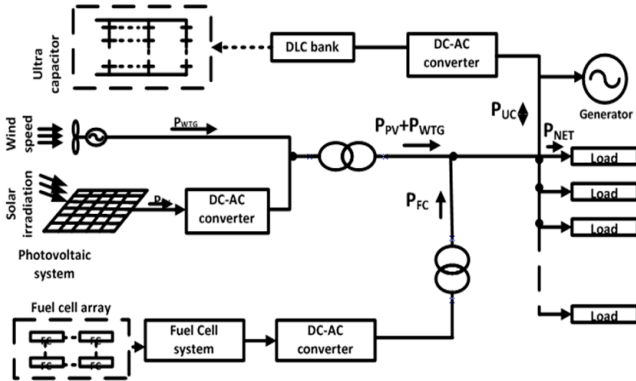


Fig. – Schematic diagram of hybrid power generation/energy storage system.

This paper devoted to compute delay margins based on specified phase and gain margins in hybrid power systems. The GPMT [24] is included in the analysis of the time-delayed hybrid LFC model as a “virtual compensator” in the feed forward part of the hybrid LFC model to analyze the gain-phase margins. Delay margin computation of hybrid LFC system that meets desired dynamic response is done by using the exact method reported in [25].

2. MODIFIED HYBRID LFC MODEL WITH GPMT

The block diagram of power generation (PG)/power distribution system is shown in Fig.1. In the proposed

design, there are three types of power generator, namely; wind turbine, photovoltaic panel and a diesel generator. Fuel cell array and ultra-capacitors are used for storage of excess energy purposes. For the stability analysis, the characteristic equation given below of hybrid LFC system with time delay is required [21]. The characteristic equation of the LFC system that is given in figure 1 with time delay is as the following

$$\Delta(s, \tau) = P(s) + Q(s)e^{-s\tau}, \quad (1)$$

where τ is time delay, and $Q(s)$, $P(s)$ are polynomials in s . These polynomials have real coefficients and are given in (2). The time delay effect is clearly indicated in block diagram of the hybrid LFC system in Fig. 2.

$$\begin{aligned} P(s) &= p_6s^6 + p_5s^5 + p_4s^4 + p_3s^3 + p_2s^2 \\ Q(s) &= q_4s^4 + q_3s^3 + q_2s^2 + q_1s \end{aligned}, \quad (2)$$

where p_i 's and q_i 's, are constants of multiplication.

In (2), M , D , T_{PV} , T_{FC} , T_{WTG} , and T_{UC} , represent the generator moment of inertia, damping coefficient of generator, time constants of the PV cells, fuel cell, wind turbine generator and ultra-capacitor respectively. A gain and phase margins tester (GPMT) as a “virtual compensator” is added to the feed forward path in control loop of the hybrid LFC system as shown in Fig. 2. The form of GPMT is given as:

$$C(A, \Phi) = Ae^{-j\phi}, \quad (3)$$

where ϕ and A represent phase and gain margins, respectively. The characteristic equation of the hybrid LFC system with the GPMT given in Fig. 2 is first obtained as,

$$\Delta(s, \tau) = P(s) + Q(s)e^{-s\tau} Ae^{-j\phi} = 0 \quad (4)$$

Let $s = j\omega_c$, $P(s) = a'_0(s)$ and collect exponential term multiplication constant as $a'_0(s)$ then eq. 4 becomes,

$$\Delta(j\omega_c, \tau) = a'_0(j\omega_c) + a'_1(j\omega_c)e^{-j\omega_c\tau} = 0. \quad (5)$$

Note that the terms $e^{-s\tau}$ and $e^{-j\phi}$ are combined to get simple exponential term in (5). The root of (5) on the imaginary axis is $s = j\omega_c$.

3. DELAY MARGIN COMPUTATION BASED ON PHASE AND GAIN MARGINS

The characteristic equation of the modified hybrid LFC system's roots on the imaginary axis for a finite time delay, is known as the delay margin stability of the modified hybrid LFC system. For that reason, first of all, the roots of the modified hybrid LFC system $s = \pm j\omega_c$ and the corresponding delay margin τ' must be computed. Next, using the imaginary roots and delay margin τ' , for desired gain and phase margins are determined. The modified hybrid LFC system is said to be asymptotically stable, if the characteristic eq. (4) has the roots, which lie in the left half of the complex plane. Finding roots of the characteristic eq. (4) has roots (if any) on the imaginary axis is known as the delay margin problem. It is known in control theory that

if the roots of any characteristic equation lie on imaginary axis then system is said to be marginally stable. Let's assume that one of the roots of characteristic equation $\Delta(j\omega_c, \tau')$ is on the imaginary axis at $s = j\omega_c$ for some finite values of the τ' . Imaginary roots have complex conjugate symmetry. Due to this symmetry property, for the same time delay τ' , the equation $\Delta(-j\omega_c, \tau') = 0$ will also have the same root at $s = j\omega_c$.

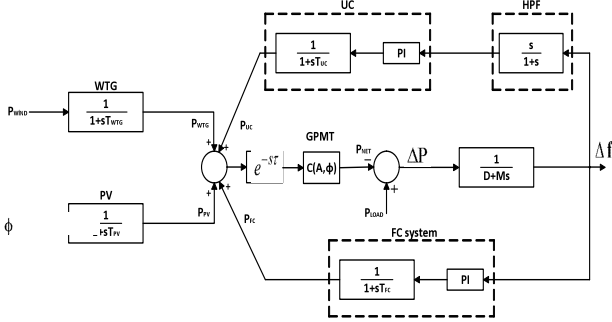


Fig. 2 – Modified block diagram of hybrid power generation/storage system with a GPMT.

As a result of this property, the problem formulation now reduces to determining values of τ' such that both equations, $\Delta(j\omega_c, \tau') = 0$ and $\Delta(-j\omega_c, \tau') = 0$ have a common root at $s = j\omega_c$. This condition can be met as follows:

$$\begin{aligned} a'_0(j\omega_c) + a'_1(j\omega_c)e^{-j\omega_c\tau'} &= 0 \\ a'_0(-j\omega_c) + a'_1(-j\omega_c)e^{j\omega_c\tau'} &= 0 \end{aligned} \quad (7)$$

The exponential terms in (7) can be cancelled out easily and a new form of characteristic equation is derived as follows:

$$W(w_c^2) = a'_0(j\omega_c)a'_0(-j\omega_c) - a'_1(j\omega_c)a'_1(-j\omega_c) = 0. \quad (8)$$

After some manipulations of the characteristic equation, the new one in terms of system parameters are obtained as:

$$W(w_c^2) = t_{12}w_c^{12} + t_{10}w_c^{10} + t_8w_c^8 + t_6w_c^6 + t_4w_c^4 + t_2w_c^2 \quad (9)$$

where t_{ij} constants of multiplication.

As we can see from (9) that it does not contain any exponential term. So, the characteristic equation in (5) which has exponential term is now converted into an ordinary equation form without using any approximation. For this reason, the imaginary roots of (5), $s = \pm j\omega_c$ coincide with the positive real roots of (9), $\omega_c > 0$, exactly.

Let's assume that the characteristic equation has a root ω_c , which is positive real, the corresponding value of τ' of the modified hybrid LFC system can be computed easily using (5) as the following,

$$\begin{aligned} \Delta(j\omega_c, \tau') &= a'_0(j\omega_c) + a'_1(j\omega_c)e^{-j\omega_c\tau'} = 0 \\ e^{-j\omega_c\tau'} &= \cos(\omega_c\tau') - j\sin(\omega_c\tau') = -\frac{a'_0(j\omega_c)}{a'_1(j\omega_c)} \\ \cos(\omega_c\tau') &= \text{Re}\left\{-\frac{a'_0(j\omega_c)}{a'_1(j\omega_c)}\right\} \\ \sin(\omega_c\tau') &= \text{Im}\left\{-\frac{a'_0(j\omega_c)}{a'_1(j\omega_c)}\right\} \end{aligned} \quad (10)$$

$$\tau' = \frac{1}{\omega_c} \tan^{-1}\left(\frac{k_9w_c^9 + k_7w_c^7 + k_5w_c^5 + k_3w_c^3}{k_{10}w_c^{10} + k_8w_c^8 + k_6w_c^6 + k_4w_c^4}\right) + \frac{2r\pi}{\omega_c} \quad (11)$$

$$r = 0, 1, 2, \dots, \infty,$$

where k_{ij} constants of multiplication. It must be noted that, for all $\tau' \in \mathcal{R}^+$, the new characteristic polynomial of (8) often have only a finite number of positive real roots. The maximum number of positive real roots is often limited to three. The set of those real roots could be shown as the following:

$$\{w_c\} = \{w_{c1}, w_{c2}, \dots, w_{cq}\}. \quad (12)$$

For each real positive root w_{cq} , $q = 1, 2, \dots, m$, the corresponding τ' could be computed by (11). These τ' values constitute a set of periodically spaced, infinitely many delay margins.

After finding the delay margin of the modified hybrid LFC system, one can easily obtain the time delay value for original hybrid LFC system. To meet these delay values, the original hybrid LFC system will have the gain and phase margins, which we are looking for. The relation between time delays is as follows: $\tau' = \tau - \frac{\phi}{\omega_c}$ here ϕ is the desired phase margin and ω_c represents the root crossing frequency. Finally, using this relationship in original systems' characteristic equation, we can get

$$\begin{aligned} \tau &= \frac{1}{\omega_c} \tan^{-1}\left(\frac{k_9w_c^9 + k_7w_c^7 + k_5w_c^5 + k_3w_c^3}{k_{10}w_c^{10} + k_8w_c^8 + k_6w_c^6 + k_4w_c^4}\right) - \\ &-\frac{\phi}{\omega_c} + \frac{2r\pi}{\omega_c}, \quad r = 0, 1, 2, \dots, \infty. \end{aligned} \quad (13)$$

3.1 STABILITY REGION BASED GAIN / PHASE MARGIN ANALYSIS

The stability region boundary can be obtained by substituting $s = j\omega_c$ into the characteristic equation in (5). Substituting $e^{-j\omega_c\tau'} = \cos(\omega_c\tau') - j\sin(\omega_c\tau')$ into (5) and separating into the imaginary and real parts characteristic equation transforms to the following form,

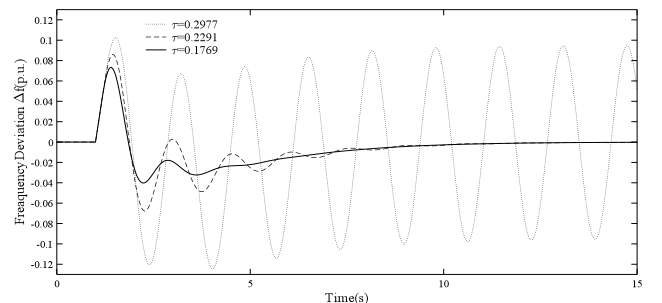


Fig. 3 – Gain margin damping effect on the frequency response for $A = 1, \phi = 0; A = 2, \phi = 0; A = 1, \phi = 15$ and $K_p = 1, K_i = 1$

The real and imaginary parts of $\Delta(j\omega_c, \tau')$ in (14) is set to zero, and the result is as

$$\begin{aligned} K_p A_1(w_c) + K_i B_1(w_c) + C_1(w_c) &= 0, \\ K_p A_2(w_c) + K_i B_2(w_c) + C_2(w_c) &= 0, \end{aligned} \quad (15)$$

where A, B, C are constants of multiplication.

$$\begin{aligned} \Delta\left(jw, \left(\tau + \frac{\phi}{w_c}\right)\right) &= K_p \left[w^4 (T_{FC} + T_{UC}) \cos w \left(\tau + \frac{\phi}{w_c}\right) - w^3 (2 + T_{UC}) \sin w \left(\tau + \frac{\phi}{w_c}\right) - w^2 \cos w \left(\tau + \frac{\phi}{w_c}\right) \right] \\ &+ K_I \left[-w^3 (T_{FC} + T_{UC}) \sin w \left(\tau + \frac{\phi}{w_c}\right) - w^2 (2 + T_{UC}) \cos w \left(\tau + \frac{\phi}{w_c}\right) + w \sin w \left(\tau + \frac{\phi}{w_c}\right) \right] \\ &- p_6 w^6 + p_4 w^4 - p_2 w^2 + j \left\{ \begin{aligned} &K_p \left[-w^4 (T_{FC} + T_{UC}) \sin w \left(\tau + \frac{\phi}{w_c}\right) - w^3 (2 + T_{UC}) \cos w \left(\tau + \frac{\phi}{w_c}\right) + w^2 \cos w \left(\tau + \frac{\phi}{w_c}\right) \right] \\ &+ K_I \left[-w^3 (T_{FC} + T_{UC}) \cos w \left(\tau + \frac{\phi}{w_c}\right) + w^2 (2 + T_{UC}) \sin w \left(\tau + \frac{\phi}{w_c}\right) + w \cos w (2 + T_{UC}) \right] + p_5 w^5 - p^3 w_3 \end{aligned} \right\} \end{aligned} \quad (14)$$

Simultaneous solution of two equations in (15) results in the stability boundary locus $\ell(K_P, K_I, \omega_c)$ of the hybrid LFC system, in the plane of (K_I, K_P) .

$$\begin{aligned} K_P &= \frac{B_1(w_c)C_2(w_c) - B_2(w_c)C_1(w_c)}{A_1(w_c)B_2(w_c) - A_2(w_c)B_1(w_c)} \\ K_I &= \frac{A_2(w_c)C_1(w_c) - A_1(w_c)C_2(w_c)}{A_1(w_c)B_2(w_c) - A_2(w_c)B_1(w_c)} \end{aligned} \quad (16)$$

As one can see, for $K_I = 0$ that a real root of $\Delta(s, \tau) = 0$ given in (16) crosses the imaginary axis at $s = j\omega_c = 0$. This corresponds to that the line $K_I = 0$ is in the boundary locus. Therefore, the stability boundary locus, $\ell(K_P, K_I, \omega_c)$ and the line $K_I = 0$ divide (K_I, K_P) -plane into two regions, namely unstable and stable regions. This part of the boundary locus is said to be the Real Root Boundary (RRB). On the other hand the boundary locus, which is determined from (16) is known as the Complex Root Boundary (CRB) of the stability region.

4. RESULTS

In this section, delay margin results and relative stability regions based on gain and phase margins of the hybrid LFC system is presented. The parameters of the hybrid LFC system and values are chosen as; time constant of WTG system, T_{WTG} : 1.5 sec.; time constant of FC system, T_{FC} : 0.26 sec.; time constant of PV system, T_{PV} : 1.8 sec.; time constant of UC system, T_{UC} : 0.01 sec. Simulations are done in Matlab/Simulink environment.

4.1. DELAY MARGIN ANALYSIS RESULTS

Delay margins that ensure stability of the hybrid LFC system for desired gain and phase margins are computed using (7) and (8) for a large set of PI controller gains. Firstly, to see the effect of the gain on delay margin the phase of hybrid LFC system ϕ is set to zero and the gain is chosen as $A = 1$ for Table I.

Table I presents the condition $A = 1$ and $\phi = 0$, which means that hybrid LFC system has no gain, no phase difference. Results show that for a fixed K_P , τ decreases as K_I increases. This indicates that the increase of K_I causes a less stable hybrid LFC system. The impact of K_P on τ has

two different patterns when K_I is fixed. For all values of K_I , τ increases as K_P increases when K_P lies in an interval of $K_P = 0-0.4$. However, τ decreases with the increase in K_P for $K_P \geq 0.6$. Such an effect K_P on τ has also been noted in excitation control systems with the time-delay, in the results of one-area LFC system [25], and in [18].

Table 1.

Delay margin results for $A = 1$ and $\phi = 0$.

τ (s)	K_I								
K_P	0.5	1	1.5	2	2.5	3	3.5	4	4.5
0.5	.518	.334	.233	.172	.132	.104	.083	.068	.056
1	.338	.297	.259	.226	.198	.174	.154	.137	.123
1.5	.246	.232	.218	.205	.192	.179	.167	.157	.146
2	.196	.189	.183	.176	.170	.164	.157	.151	.145
2.5	.164	.160	.157	.153	.150	.146	.142	.139	.135
3	.141	.139	.137	.135	.133	.130	.128	.126	.124
3.5	.125	.123	.122	.120	.119	.117	.116	.114	.113
4	.111	.110	.109	.108	.107	.106	.105	.104	.103
4.5	.101	.100	.099	.098	.098	.097	.096	.095	.095
5	.092	.091	.091	.090	.089	.089	.088	.088	.087

To observe tendency of delay margin, we increase the gain of hybrid LFC system a bit more, that is the gain and phase margins are selected as A from 1 to 3 and $\phi = 0$ to investigate how the delay margin is effected by only gain margin. It is observed that the increasing the gain margin results in a notably decrease in the delay margins for all PI controller gains. Secondly, to investigate how the delay margin is effected by only with changing delay margin, while the gain margin held constant, that is $A = 1$, and phase margins are selected as $\sqrt{=} 15^\circ$ and $\sqrt{=} 30^\circ$.

The result is that the increasing the phase margin till $\sqrt{=} 30^\circ$ degree a notable increase in the delay margins for all PI controller gains is observed. While above $\sqrt{=} 30^\circ$ degree a notable decrease in the delay margins for all PI controller gains is observed. When $\sqrt{=} > 0$, for a fixed K_I value, delay margin increases for a certain K_P value; than it decreases again. However, if we compare the decrease ratio in delay margins between the gain and phase margin, we can see that phase margin is affecting delay less than that of gain margin.

Finally, the simultaneous impact of the gain margin A and phase margin ϕ is also analyzed. Both gain and phase margins are varied to observe the effect on the delay margin. When time delay margins are compared, one can see that delay margin duration is decreasing with the increase of either phase or gain values.

The results show that delay margins decreases sharply for all PI controller gains when both the phase and gain margins

are considered.

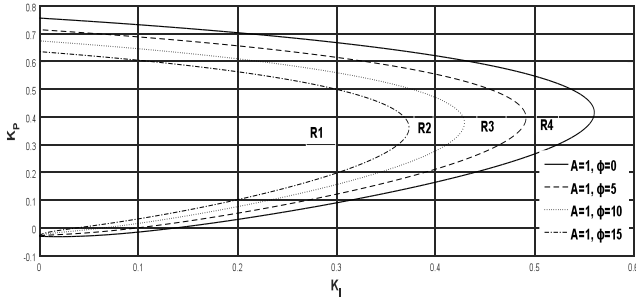


Fig. 4 – Stability region of PI controller for $A = 1$ and different ϕ .

To observe the effect of phase and/or gain margins on time delay margin we performed time-domain simulations. Figure 3 compares the frequency response of the hybrid LFC system to a load disturbance of $\Delta P_d = 0.1 pu$ for $A = 1, \sqrt{\cdot} = 0^0$, $A = 2, \sqrt{\cdot} = 0^0$ and $A=1, \sqrt{\cdot} = 15^0$ when the PI controller gains are $K_I = 1, K_P = 1$. For $A = 1, \sqrt{\cdot} = 0^0$ delay margin is found to be $\tau = 0.2977$ s. It can be seen in Fig. 3 that the hybrid LFC system shows continuous oscillations for this delay value. These sustained oscillations indicate that hybrid LFC system is marginally stable. Practically, for power systems, these types of oscillations in the frequency deviations are undesirable. So this issue should be solved.

To overcome such an unacceptable oscillation, phase and/or gain margins have to be taken into account in delay margin computation.

4.2 PHASE AND GAIN MARGINS BASED RELATIVE STABILITY REGIONS

First of all, in Fig. 4, we obtained relative stability region that depends on phase. Next, gain dependency of relative stability region is analyzed. For both, the time delay is chosen as $\tau = 0.5$ s and the range of the crossing frequency is selected as, $0 < \omega < 3$ for stability boundary locus. The aim is to find the stabilizing values of K_P and K_I such that the characteristic equation of (4) should be Hurwitz stable with expected phase and gain margins. Also, one can get the stability region considering only phase margins by substituting $A = 1$ and $\Phi = 30^0$ in eq. (17)-(19). This region is labeled as R4 in Fig. 4. As can be seen in Fig. 4 that relative stability region with constant gain is shrinking with proportional raise in phase margin. Relative stability regions are obtained as follows. Let the desired phase and gain margins are $A \geq 3$ and $\Phi \geq 30^0$ respectively. For this choice, substitute $A = 3$ and $\Phi = 30^0$ in eq. (17) to (19). As a result, crossing frequency $\omega = 2.9297$ rad/s is obtained for specified gain/phase margin. Next, in Fig. 5, controller parameters K_P and K_I 's dependency on time delay τ is analyzed and relative stability regions are obtained. As can be seen in figure 5 that 0.5 ms. raise in time delay τ causes decrease in controller parameter space drastically.

Finally, from Fig. 4 one point is selected for each region, $K_P = 0.3, K_I = 0.3$ in R1, $K_P = 0.3, K_I = 0.4$ in R2, $K_P = 0.3, K_I = 0.45$ in R3 region and $K_P = 0.3, K_I = 0.51$ in R4 region respectively. The hybrid LFC system frequency response to a load disturbance of $\Delta P_d = 0.1 pu$ is shown in Fig. 6. It can be seen that all responses are stable. Although all responses are stable, the deviation of frequency for $K_P = 0.3, K_I = 0.51$ has more oscillations than other three responses. Since it is

known in control systems that the higher the oscillations, the more vulnerable to instability. For that reason, for robust hybrid LFC system the frequency deviation should decay as fast as possible.

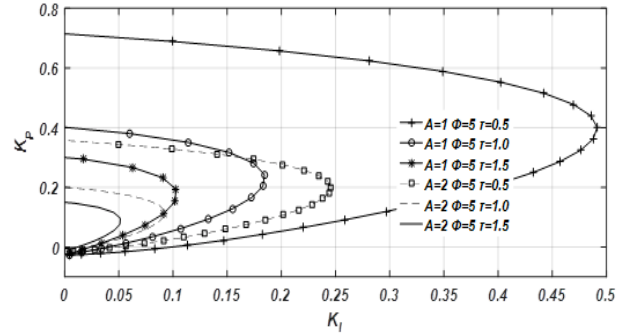


Fig. 5 – Stability region of PI controller for different τ .

If the (K_P, K_I) values are selected from inner relative stability region, the hybrid LFC system will has a non-oscillatory and quicker disturbance rejection performance. If the (K_P, K_I) values are selected from $A = 2, \sqrt{\cdot} = 5^0$ and $\tau = 0.5$ s region in Fig. 5, disturbance rejection performance of the LFC system would be slower than that of inner relative stability region.

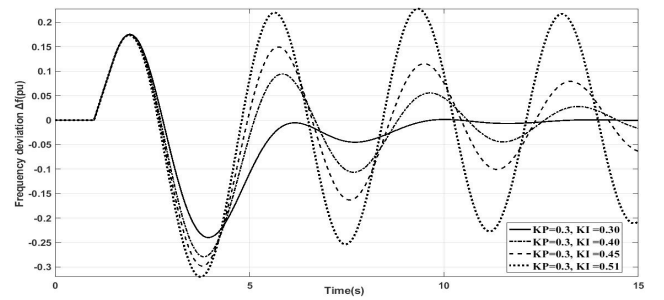


Fig. 6 – Frequency deviation responses for four different values of controller gains.

5. CONCLUSIONS

This paper has computed delay margins of the hybrid LFC system by using an analytical method. Also, to determine relative stability regions with different PI controller and gain-phase margins parameter selection, a graphical method is presented. This method is based on the determination of stability boundary locus for hybrid LFC system which has communication delay. Stability boundary locus is determined for desired location of the closed-loop roots of hybrid LFC system. The analysis that is investigated in this paper show that if delay margins are obtained considering only the stability, then it may cause unacceptable oscillations in the frequency deviation. Moreover, delay margin determination which took gain and phase margins into account, improves the dynamic response. Obtaining different relative stability regions with different parameter sets provides us an in depth sight view of controller parameter selection. The relative stability regions shows a way of selection of controller gains for the designer that ensure the time-delayed hybrid LFC system is in stable region. As a result of this paper, following comments and observations can be made:

- i. If only the stability taken into account, then delay

margins result in poor dynamic performance. Also, it results in oscillations in the frequency.

- ii. Both phase and gain margins affect the delay margins significantly.
- iii. When delay margins are decreased, then the phase and/or gain margins are increased.
- iv. While choosing delay margins, gain and phase margin values should be taken into account if a better dynamic performance is required in term of less settling time and fast damping.
- v. When phase and/or gain margins are increased, relative stability regions shrink.

With the aim of the stability region, the PI controller parameters selection could be conveniently determined such that the hybrid LFC system having communication delays will be not only stable and but also will have a desired dynamic performance in terms of settling time, damping and non-oscillatory behaviors.

Received on August 24, 2019

REFERENCES

1. Y.Sawle, et al., *PV-wind hybrid system: A review with case study*. Cogent Engineering, **3**, 1 p. 1189305 (2016).
2. S. Diaf, et al., *Design and techno-economical optimization for hybrid PV/wind system under various meteorological conditions*, Applied Energy, **85**, 10, pp. 968–987 (2008).
3. M. Pereira, D.M. de la Pena, D. Limon, *Robust economic model predictive control of a community micro-grid*. Renewable Energy, **100**, pp. 3–17 (2017).
4. P. Marcon, et al., *A Real Model of a Micro-Grid to Improve Network Stability*. Applied Sciences-Basel, **7**, 8, (2017).
5. P. Zaheeruddin, M. Manas, *Analysis of Design of Technologies, Tariff Structures, and Regulatory Policies for Sustainable Growth of the Smart Grid*. Energy Technology & Policy, **2**, 1, pp. 28–38 (2015).
6. T.J. Mary, P. Rangarajan, *Delay-dependent Stability Analysis of Microgrid with Constant and Time-varying Communication Delays*. Electric Power Components and Systems, **44**, 13, pp. 1441–1452 (2016).
7. S.C. Gupta, Y.K. Gayatri-Agnihotri, *Design of an autonomous renewable hybrid power system*. International J. of Renewable Energy Technolog, **2**, 1, pp. 86–104 (2011).
8. N Mohsenifar, A. Kargar, N.R. Abjadi, *Improved cascade sliding mode for power control in a microgrid*, Rev. Roum. Sci. Techn. - Électrotechn. et Énerg., **61**, 4, pp. 430–435 (2016).
9. H. Bevrani, T. Hiyama, *Robust decentralised PI based LFC design for time delay power systems*. Energy Conv. and Management, **49**, 2, pp. 193–204 (2008).
10. A. Elahi, A. Alfí, *Finite-time H_∞ control of uncertain networked control systems with randomly varying communication delays*. ISA Trans., **69** (Supplement C), pp. 65–88 (2017).
11. S. Elkawafi, et al. *Delay-dependent stability of LFC in Microgrid with varying time delays*, in 2016 22nd Int. Conf. on Automation and Comp. (ICAC) 2016.
12. K. Ramakrishnan, G. Ray, *Improved results on delay-dependent stability of LFC systems with multiple time-delays*, J. of Control, Automation and Electrical Systems, **26**, 3, pp. 235–240 (2015).
13. I. Serban, C. Marinescu, *Power quality issues in a stand-alone microgrid based on renewable energy*, Rev. Roum. Sci. Techn. - Électrotechn. et Énerg., **53**, 4, pp. 285–293 (2008).
14. M. Nayeripour, M. Hoseintabar, T. Niknam, *Frequency deviation control by coordination control of FC and double-layer capacitor in an autonomous hybrid renewable energy power generation system*. Renewable Energy, **36**, 6, pp. 1741–1746 (2011).
15. C.K. Zhang, et al., *Further results on delay-dependent stability of multi-area load frequency control*. IEEE Trans. on Power Systems, **28**, 4, pp. 4465–4474 (2013).
16. L. Wang, et al., *Analysis of a novel autonomous marine hybrid power generation/energy storage system with a high-voltage direct current link*. Journal of Power Sources, **185**, 2, pp. 1284–1292 (2008).
17. D.J. Lee, L. Wang, *Small-signal stability analysis of an autonomous hybrid renewable energy power generation/energy storage system part i: time-domain simulations*. IEEE Trans. on Energy Conversion, **23**, 1, pp. 311–320 (2008).
18. J. Chen, G. Gu, C.N. Nett, *A new method for computing delay margins for stability of linear delay systems*. Systems & Control Letters, **26**, 2, pp. 107–117 (1995).
19. S. Ayasun, A. Gelen, *Stability analysis of a generator excitation control system with time delays*. Electrical Engineering, **91**, 6, pp. 347–355 (2009).
20. S. Doolla, T.S. Bhatti, *Load frequency control of an isolated small-hydro power plant with reduced dump load*. IEEE Trans. on Power Systems, **21**, 4, pp. 1912–1919 (2006).
21. S.Y. Obara, *Analysis of a fuel cell micro-grid with a small-scale wind turbine generator*, Int. J. of Hydrogen Energy, **32**, 3, pp. 323–336 (2007).
22. P. Puri, S. Ghosh, *A hybrid optimization approach for PI controller tuning based on gain and phase margin specifications*. Swarm and Evolutionary Comp, **8**, pp. 69–78 (2013).
23. D.-J.Wang, *A PID controller set of guaranteeing stability and gain and phase margins for time-delay systems*, J. of Process Control, **22**, 7, pp. 1298–1306 (2012).
24. S. Sönmez, A. Saffet, *Gain and phase margins based delay-dependent stability analysis of single-area load frequency control system with constant communication time delay*, Trans. of the Institute of Measurement and Control, 2017.
25. S. Sönmez, S. Ayasun, C.O. Nwankpa, *An exact method for computing delay margin for stability of load frequency control systems with constant communication delays*, IEEE Trans. on Power Systems, **31**, 1, pp. 370–377 (2016).
26. H. Erol, S. Ayasun, *Stability analysis of time delay in hybrid power systems*, (in Turkish) Politeknik Dergisi, **23**, 4, pp. 1131–1139.